

## Structure and Mechanical Properties of PP/EPDM/Attapulgite Ternary Blends

Xiang GAO,<sup>1</sup> Li-xin MAO,<sup>1</sup> Ri-guang JIN,<sup>1</sup> Li-qun ZHANG,<sup>2</sup> and Ming TIAN<sup>2,†</sup>

<sup>1</sup>The Key Laboratory of Beijing City on Preparation and Processing of Novel Polymer Materials, Beijing University of Chemical Technology, Beijing 100029, China

<sup>2</sup>Key Laboratory for Nano-Materials, Ministry of Education, Beijing 100029, China

(Received November 20, 2006; Accepted June 20, 2007; Published August 7, 2007)

**ABSTRACT:** Polypropylene(PP)/ethylene-propylene-diene copolymer (EPDM)/fibrillar silicate attapulgite (AT) ternary blends were first prepared *via* the two-step melt blending process, by which the AT was blended with EPDM prior to compound with PP. Structure and mechanical properties of the blends were investigated. According to the analysis of TEM and DMA test, it was concluded that as for PP/EPDM/AT ternary blends, the typical “sea-island” morphology was observed, and the morphology of encapsulated structure like sandbag was formed in PP matrix besides neat EPDM dispersion domain, where EPDM encapsulated fibrillar silicate AT. The most-odds diameter ( $D_m$ ), the number-average diameter ( $D_n$ ) and the weight-average diameter ( $D_w$ ) of dispersed particles decreased with increasing EPDM. PP/EPDM/AT ternary blends showed higher yield strength and dynamic modulus than the corresponding PP/EPDM binary systems due to the reinforcement of AT. PP/EPDM/AT ternary blend (100/20/5) possessed the balanced yield strength (21.9 MPa) and impact strength (47.7 kJ·m<sup>-2</sup>), relative to 23.0 MPa and 9.4 kJ·m<sup>-2</sup> of PP. The micromechanical deformation process—mainly debonding of dispersed particles and shear yielding was mainly responsible for impact resistance of the ternary blends. [doi:10.1295/polymj.PJ2006166]

**KEY WORDS** Polypropylene / Ethylene-propylene-diene Copolymer / Attapulgite / Morphology / Properties /

Polypropylene (PP) is one of the most widely used polyolefin polymers. The toughening has been one of the most active and significant theme in the field of the modification for PP resin. Ethylene-propylene copolymer (EPR) or ethylene-propylene-diene copolymer (EPDM) copolymer has been often used to toughen PP. At present, the impact strength of the modified resin can be enhanced by four times relative to the matrix by adding elastomers.<sup>1,2</sup> Unfortunately, the enhancement of the toughness is obtained at the expense of the stiffness, elastic modulus, and thermal resistance. In recent years, ternary phase blends of PP containing soft elastomer and rigid fillers are of ever-increasing interest because both their stiffness and toughness can be partly controlled and materials with balanced mechanical properties can be formulated. So far, various fillers to increase stiffness have been employed in ternary polypropylene blends, which include talc,<sup>3,4</sup> calcium carbonate<sup>5,6</sup> and kaolin,<sup>7</sup> etc.

Attapulgite (AT) is a type of natural fibrillar silicate clay mineral. There are large reserves of AT in South China (Jiangsu, Zhejiang, and Anhui province) and in USA (Florida). The chemical structure of AT is Mg<sub>5</sub>Si<sub>8</sub>O<sub>20</sub>(OH)<sub>2</sub>(OH<sub>2</sub>)<sub>4</sub>·4H<sub>2</sub>O. The smallest structure unit of AT is fibrillar single crystal with a length of 500–2000 nm and 10–25 nm in diameter.<sup>8,9</sup> Unlike the layer-layer interaction existing in layered silicates,

the interaction between AT single crystals is extremely small due to a similar line-line contact, which could result in a weak interaction and facilitate the separation of AT micro-agglomerates into single crystals upon large shear and physical and chemical modification. By polymer melt blending or *in-situ* polymerization, AT could also be separated into lots of nanosized fibrils with high aspect ratio, showing effective reinforcement for polymer.<sup>10–12</sup>

In this paper, the ternary blends of PP/EPDM/AT were first prepared *via* two-step melt blending process, in which AT was blended with EPDM to make master batch first and then the master batch of EPDM/AT was compounded with PP. The structure morphology of the ternary blends was observed by transmission electron microscope (TEM) and scanning electron microscope (SEM). The diameter of the dispersed particles in the ternary blends was calculated based on the statistic data *via* the image analyzer. Also, the mechanical properties of the blends were discussed.

### EXPERIMENTAL

#### Materials

Attapulgite powder (particle size, 2–5 micron) was obtained from Dalian global minerals company of

<sup>†</sup>To whom correspondence should be addressed (Tel: 8610-64434860, Fax: 8610-64433964, E-mail: tianm@mail.buct.edu.cn).

China. The matrix material for the blends was commercially available polypropylene (PP) homopolymer 1300 [melt flow rate (MFR) = 1.0 g/10 min, density  $\rho = 0.90 \text{ g/cm}^3$ ] from Yanshan Petrochemical Co., China. The elastomer was EPDM (EP-33) consisting of 33 wt% propylene with the density  $\rho = 0.85 \text{ g/cm}^3$ , which is product of JSR Co., Japan. The hydrophilic silane coupling agent AG-102 was the product of Nanjing Shuguang Chemical Plant., China.

#### Preparation of organically modified AT

50 g AT was dispersed into 1000 mL hot water using stirrer. 2.5 g silane coupling agent AG-102 was dissolved in hot water (200 mL) and then poured into the AT water suspension under vigorous stirring for 1.5 h. The product was filtered off and washed three times. Treated AT was dried in a blast oven at  $105^\circ\text{C}$  for 1.5 h, and then was ground to get the final powder. Before use, the powder was screened by 1250-mesh screen.

#### Preparation of ternary blends

The ternary blends of PP/EPDM/AT were prepared *via* two-step melt blending process, in which AT was blended with EPDM to make master batch first, and then compounded with PP.

The master batch of EPDM/AT (100/50) was prepared using a two-roll mill. The EPDM was put into the two-roll mill first, adjusting the two rolls to the smallest distance when EPDM become soft. AT was then slowly added into EPDM to ensure good dispersion. The time of mixing was 15~25 min.

The above master batch was blended with PP, EPDM using a co-rotating twin-screw extruder with an L/D ratio of 45 and screw diameter of 35 mm (ZSK-25WLE, WP Co., Germany). Additional EPDM was introduced to control the blend ratio of PP/EPDM/AT system. The temperature profiles of the barrel were  $210^\circ\text{C}$ ,  $215^\circ\text{C}$ ,  $225^\circ\text{C}$ ,  $225^\circ\text{C}$ ,  $220^\circ\text{C}$  from the hopper to the die, and the screw speed was 150 rpm. The extruded pellets were injection-molded into standard test samples in a CJISONC—II (China) injection-molding machine. The temperature profiles were  $200^\circ\text{C}$ ,  $220^\circ\text{C}$  and  $215^\circ\text{C}$  from hopper to die. In this paper, the composition of the blends is representing the mass fraction.

#### Characterization

Tensile strength was measured according to ASTM D-638 using an Instron tensile machine (Instron 1185, USA). The crosshead speed was set as 50 mm/min in all experiments. The Izod impact test of notched specimens was carried out on a XJU-2.75 impact tester, according to ASTM D-256. All measurements were performed at room temperature and the

average of five measurements for each specimen was reported.

The morphology structure of ternary blend was observed by transmission electron microscope (TEM) and scanning electron microscope (SEM). The ultrathin sections were cut from the injection-molded sample in liquid nitrogen, and were stained with osmium tetroxide ( $\text{OsO}_4$ ) to obtain sufficient contrast between dispersion phase and PP matrix. A Hitachi (Japan) H-800 TEM with an acceleration voltage of 100 kv was used to observe the ultrathin sections. The morphology of fracture surface of impact test pieces was observed with a Cambridge (British) S-250MK3 SEM. The fracture surfaces were vacuum-plated with gold-platinum for electrical conducting.

Samples for dynamic mechanical analysis (DMA) were cut from the gauge length of injection molded tensile bars and were  $\sim 4 \text{ cm}$  long,  $\sim 1.2 \text{ cm}$  wide and  $\sim 0.4 \text{ cm}$  thick. DMA was performed using a Rheometrics ARES-V rheometer (USA) in bend configuration at a frequency of 1 Hz. The temperature range was  $-100^\circ\text{C} \sim 100^\circ\text{C}$ . The heating rate was  $5^\circ\text{C}/\text{min}$ .

The calculation of the sizes of dispersed particles for the PP/EPDM/AT blends: based on tens of TEM images for the PP/EPDM/AT blends, the size of the smallest dimension of each dispersed particle in the dispersion domain was analyzed and measured by using the image analyzer. The most-odds diameter ( $D_m$ ) was obtained by the analysis of the above measured data. The number-average diameter ( $D_n$ ) and the weight-average diameter ( $D_w$ ) were individually calculated by the formula as following:

$$D_n = \frac{\sum_i n_i d_i}{\sum_i n_i} \quad D_w = \frac{\sum_i n_i d_i^2}{\sum_i n_i d_i}$$

Here  $d_i$  means the diameter of the dispersed particle with the order of  $i$ ;  $n_i$  means the number of the dispersed particle with the diameter of  $d_i$ .

## RESULTS AND DISCUSSION

#### Morphology of PP/EPDM/AT ternary blends

TEM micrographs of the PP/EPDM/AT ternary blends are shown in Figure 1. Two-phase morphology, *i.e.* "sea-island" morphology was clearly visible in both systems, in which there were two different dispersed domains (dark part) and one continuous domain (gray part). Gray parts indicated PP as a continuous domain. The light-dark spherical particles with less than  $1 \mu\text{m}$  designated neat EPDM dispersion phase originated from additional EPDM, whereas the irregular dark particles with more than  $1 \mu\text{m}$  designated EPDM/AT dispersed phase originated from AT filled EPDM master batch, as shown in Figure 1.

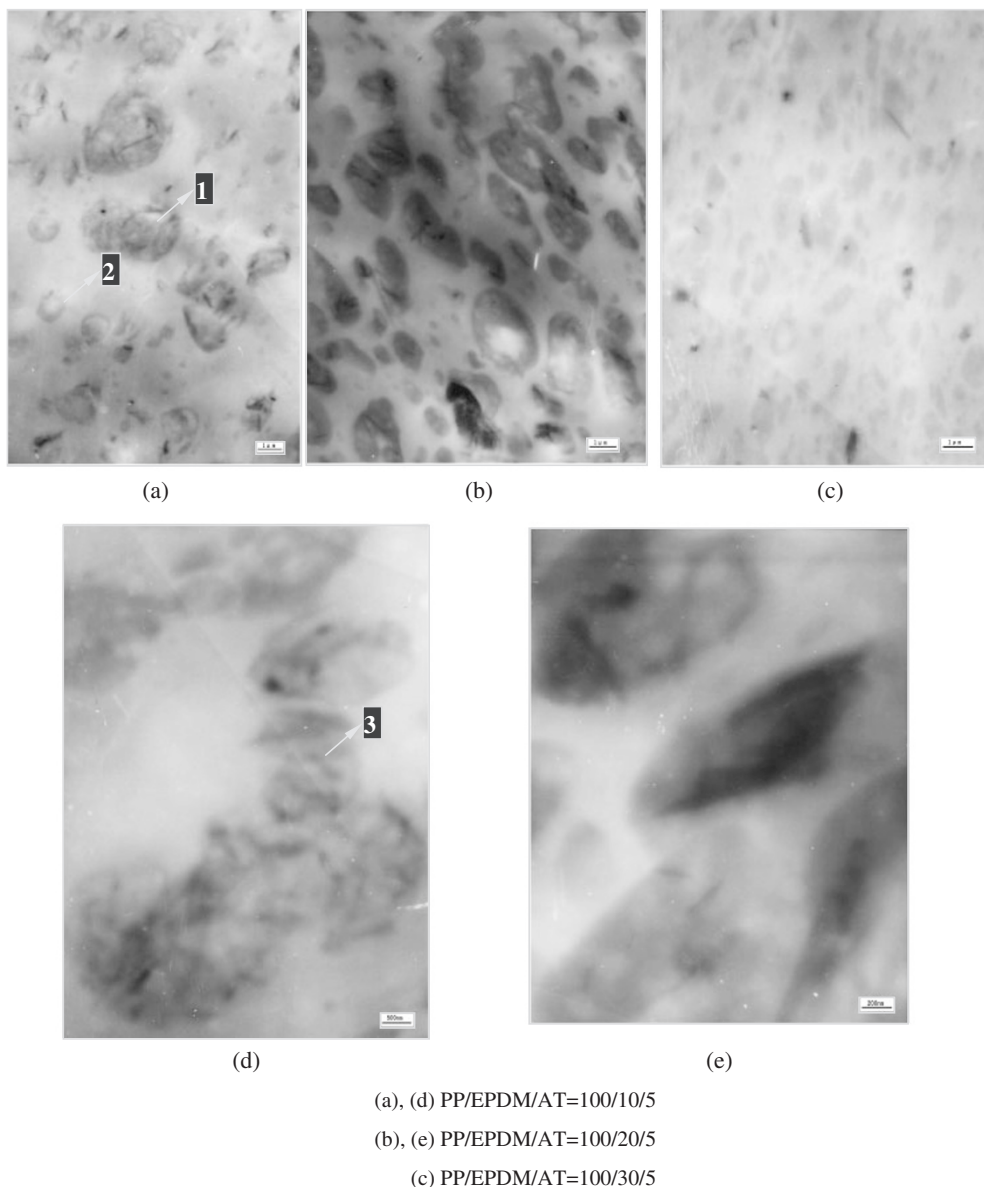


**Figure 1.** TEM photographs of PP/EPDM/AT (1. dispersed EPDM/AT particle; 2. dispersed EPDM particle; 3. AT single crystals).

It was due to that the introduction of AT remarkably increased the viscosity of EPDM (50/50), resulting in the increase in EPDM/AT domain size, much larger than that of neat EPDM particle. An increase of EPDM content in the system did not change this two-phase morphology but increased the number of dispersed EPDM particles in the PP matrix. It seemed that the size of the dispersed domain decreased. It was worth noting that the crystal bundles or micro-agglomerating particles of AT were hardly visible in the PP phase rather than presented in EPDM/AT particles. Figure 1d–e further shows the morphology of EPDM/AT particles in the PP matrix and the inter-phase region in the ternary blends. It could be observed that an encapsulation structure like sand-bag was achieved in the ternary system, where the rubber encapsulated AT to form core-shell inclu-

sion, and AT in the EPDM was separated as crystal bundles, and even fibrillar single crystals to construct a filler network. Also, there were a lot of interstice spaces among these loose-stacking single crystals and crystal bundles.

The phase structure of ternary blends is influenced by many factors, including the surface characteristics, blend ratio, melt rheology of the system and compounding techniques.<sup>13</sup> When new surfaces and interfaces are created, the input of some energy is required and the system tends to acquire a type of morphology with a minimum surface free energy. Thermodynamic analysis revealed that encapsulation was the thermodynamically controlled process.<sup>14</sup> The morphology of encapsulation was also reported in the PP/EPR/calcium carbonate<sup>5</sup> and PP/EVA/calcium carbonate<sup>8</sup> ternary systems. The reason for the filler encapsula-

**Table I.** Average diameter of dispersed particles of PP/EPDM/AT blends

PP/EPDM/AT composition	Most-odds diameter ( $D_m$ ) $\mu\text{m}$	Number-average diameter ( $D_n$ ) $\mu\text{m}$	Weight-average diameter ( $D_w$ ) $\mu\text{m}$
100/5/5	0.566731	0.555070	0.5761
100/10/5	0.298951	0.322066	0.3348
100/20/5	0.206958	0.204475	0.2163
100/30/5	0.152889	0.155509	0.1597

tion by elastomer is that the formation of interface between the PP matrix and filler particles, *i.e.* between components with the lowest and the highest surface energy, reduces the sum of interfacial energies in a volume unit of the blend.<sup>15</sup> For the PP/EPDM/AT ternary system in this study, such an introduction sequence of the compositions increased the tendency of rubber particles adhere to the AT surface, in which the AT was mixed with EPDM firstly, and then EPDM/AT master batch was blended with PP. Hence, an encapsulation structure was finally formed in the ternary PP/EPDM/AT blends. Also, it was to be noted that the Si-OH of silane coupling agents after being hydrolyzed could react with the hydroxyl groups of AT,<sup>12</sup> which decreased the surface free energy of AT and improved the adhesion between AT and EPDM, and therefore the stability of the encapsulate units against shear forces during the mixing process was enhanced.<sup>14</sup>

Table I displays the average diameter of dispersed particle of PP/EPDM/AT blends. The extra EPDM was added into the other blends except PP/EPDM/AT (100/5/5) blend. Since the diameters in Table I were obtained by measuring the size of the smallest dimension of each dispersed particle, they were much smaller than those observed in Figure 1. Seen from Table I, the most-odds diameter ( $D_m$ ), the number-average diameter ( $D_n$ ) and the weight-average diameter ( $D_w$ ) of the dispersed particles in PP/EPDM/AT ternary blends decreased with increasing EPDM. The more decrease was observed as the EPDM content increased from 5 phr (per hundred PP) to 10 phr in the blends. This trend agreed with the observations in Figure 1. As afore-discussion, dispersed EPDM particles had smaller sizes than EPDM/AT dispersed particles, and the increase of EPDM increased the number of dispersed EPDM particles, leading to the decrease of  $D_m$ ,  $D_n$  and  $D_w$ .

#### Mechanical properties of blends

The mechanical properties of PP/EPDM blends and PP/EPDM/AT ternary blends are shown in the Table II respectively, in which the composition of each system correspond to the mass of EPDM or AT added to PP matrix.

**Table II.** Effect of the compositions on mechanical properties of polypropylene/EPDM/AT ternary blends

Composition PP/EPDM/AT	$IS^a$ ( $\text{kJ}\cdot\text{m}^{-2}$ )	$S_{yc}^b$ (MPa)
<b>System1</b>		
100/0/0	$9.4 \pm 0.1$	$23.0 \pm 0.2$
100/5/0	$15.5 \pm 0.2$	$21.4 \pm 0.2$
100/10/0	$35.5 \pm 0.4$	$20.1 \pm 0.2$
100/15/0	$47.2 \pm 0.5$	$19.5 \pm 0.2$
100/20/0	$49.5 \pm 0.5$	$17.8 \pm 0.2$
100/30/0	$51.2 \pm 0.5$	$14.5 \pm 0.2$
<b>System2</b>		
100/0/5	$7.6 \pm 0.1$	$25.9 \pm 0.3$
100/5/5	$12.8 \pm 0.1$	$24.3 \pm 0.2$
100/10/5	$37.5 \pm 0.4$	$23.1 \pm 0.2$
100/15/5	$44.5 \pm 0.4$	$22.8 \pm 0.2$
100/20/5	$47.7 \pm 0.5$	$21.9 \pm 0.2$
100/30/5	$49.0 \pm 0.5$	$18.2 \pm 0.2$
<b>System3</b>		
100/20/0	$49.5 \pm 0.5$	$17.8 \pm 0.2$
100/20/1	$51.1 \pm 0.5$	$18.5 \pm 0.2$
100/20/3	$53.7 \pm 0.5$	$19.1 \pm 0.2$
100/20/5	$47.7 \pm 0.5$	$21.9 \pm 0.2$
100/20/7	$42.9 \pm 0.4$	$20.9 \pm 0.2$
100/20/9	$35.5 \pm 0.4$	$21.4 \pm 0.2$

<sup>a</sup>Izod impact strength of blends. <sup>b</sup>Yield stress of blends.

**Yield stress and tensile properties.** Yield stress is an important characteristic of polymeric materials because it indicates the limits of allowable tensile stress in engineering application. The yield stress of the PP matrix is  $S_{yc} = 23.0$  MPa (Table II). It could be seen from System1 and System2 that the values of  $IS$  were enhanced with the increasing introduction amount of EPDM into PP matrix, whereas the  $S_{yc}$  were dramatically reduced. For instance, the incorporation of 20 wt% EPDM caused the yield stress to drop to 17.8 and 21.9 MPa for the binary PP/EPDM and ternary PP/EPDM/AT systems respectively. The reason was attributed to that the droplets of EPDM dispersed in the PP matrix are too weak to sustain stress of continuous phase. Furthermore, it should be noticed that the yield stress for ternary PP/EPDM/AT system was higher than the binary PP/EPDM system at the same EPDM loading. For the ternary system (System3) with a given blend ratio of PP and EPDM (100/20),  $S_{yc}$  increased with the increasing amount of AT. As previously described, AT was separated into single crystals or loose-stacking crystal bundles in the EPDM droplets with an encapsulation structure and still keep a relatively high aspect ratio. Therefore, AT showed pronounced reinforcing effect for the EPDM dispersion phase to sustain the stress, as a result, the strength of ternary blends was greatly enhanced.

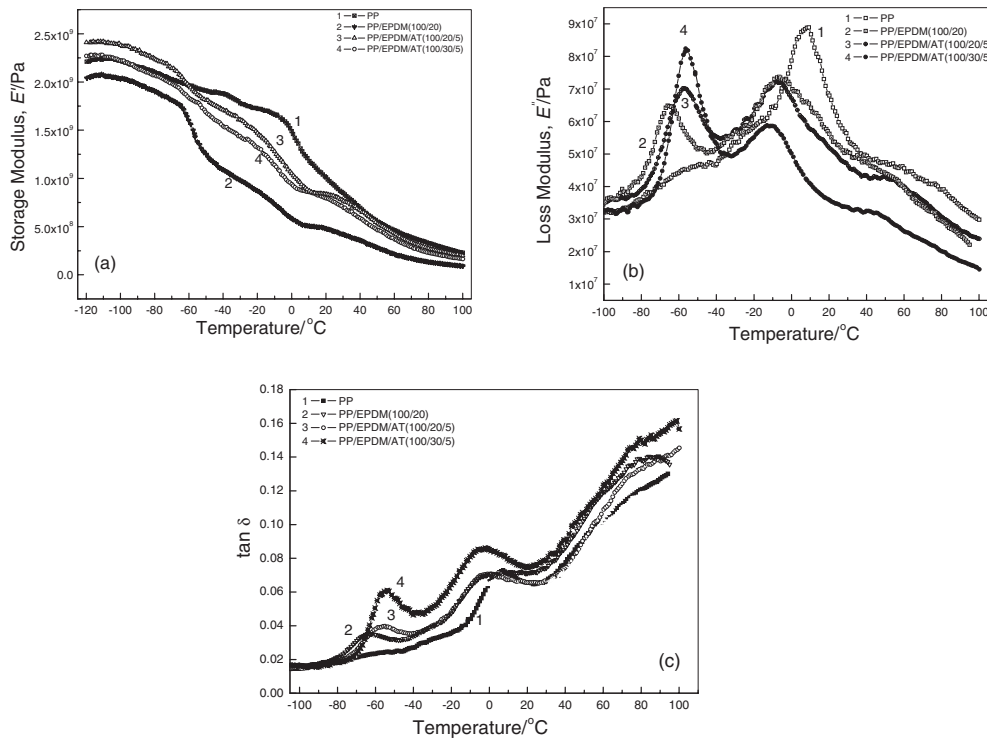


**Figure 2.** The temperature dependence of dynamic mechanical behavior for PP, PP/EPDM, PP/EPDM/AT.

**Izod impact strength and toughness.** It could be seen from System1 and System2 that EPDM showed pronounced improvement in impact resistance for the PP matrix, which was consistent with the results reported in literatures.<sup>1,2</sup> For the ternary blends (System3) with a given ratio of PP and EPDM (100/20), *IS* was also improved by about 10%, if 1~3 wt % of AT was incorporated. However, the evident decrease in the impact strength of ternary blends could be found when the incorporation amount of AT was more than 5 wt%. This implied that there was a synergistic toughening effect of EPDM and AT together in the ternary blends with the morphology of encapsulation, as has been reported in the literature.<sup>16</sup> From the above results, it could be concluded that the enhancement of the toughness was obtained at the expense of the yield stress for a binary blend of PP/EPDM. However, both their strength and toughness may be partly controlled and the materials with balanced mechanical properties may be achieved for the ternary phase blends based on PP containing soft elastomer and rigid AT together. For an example, compared with the sample (100/20), although the impact strength was decreased by 1.8 kJ·m<sup>-2</sup>, yield strength of the sample (100/20/5) was raised by 4.1 MPa. Relative to neat PP, the impact strength of ternary blend (100/20/5) was enhanced by 4 times, but yield strength only decreased 1.1 MPa; the impact strength of ternary blend (100/10/5) was enhanced by 3 times without any expense of yield strength, demon-

strating that ternary PP/EPDM/AT blends possessed even better overall mechanical properties.

#### Dynamic mechanical properties

The dynamic mechanical properties of PP, PP/EPDM blends, and PP/EPDM/AT ternary blends were determined by DMA techniques. The temperature dependence of storage modulus  $E'$ , loss modulus  $E''$  and  $\tan \delta$  at 1 Hz are shown in Figure 2a–c respectively.

It's shown in Figure 2a that  $E'$  of the pure PP was higher than that of PP/EPDM blends, resulted from the addition of elastomer EPDM with lower modulus relative to PP matrix. It can be seen clearly that PP/EPDM/AT hybrids had higher  $E'$  values than that of PP/EPDM system over whole temperature range, demonstrating the reinforcement effects of AT fibrillar crystals. From Figure 2b, one can see that the  $E''$  peaks of PP/EPDM blend and PP/EPDM/AT ternary blend was higher than that of PP at about  $-60^\circ\text{C}$ , which may be mainly attributed to the energy dissipation of dispersion phase, including the inter-chain friction of EPDM, inter-phase friction between EPDM and AT crystals, and between loose-stacking crystal bundles. However,  $E''$  peaks for the former two systems was remarkably lower than that for PP at about  $0^\circ\text{C}$ , which may be mainly attributed to the energy dissipation of continuous phase (PP).

Figure 2c shows the temperature dependence of the loss factor for the blended systems. The loss factor of

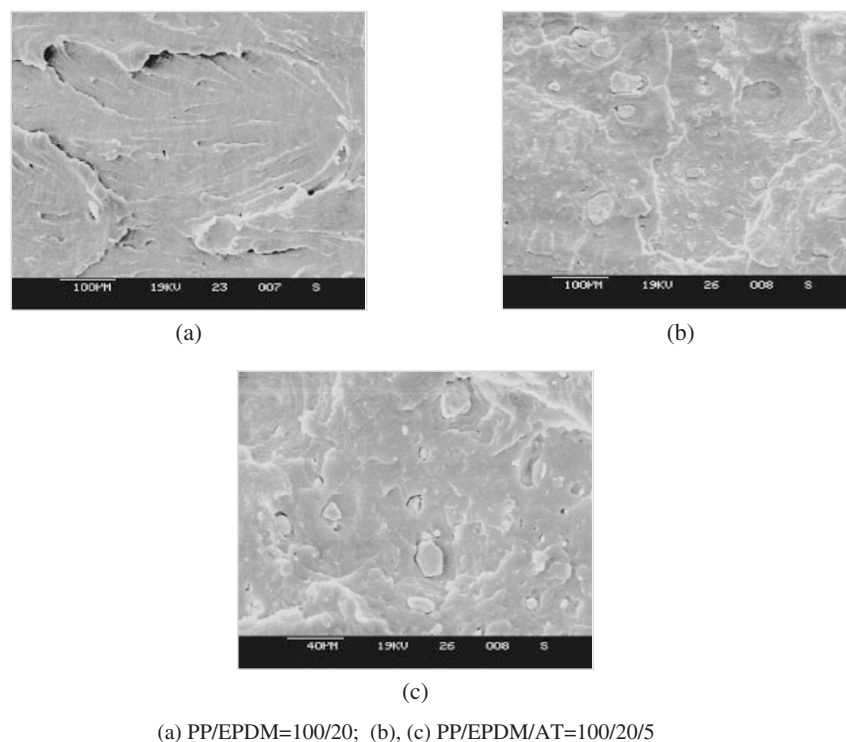


**Figure 3.** The impact fracture morphology of PP/EPDM and PP/EPDM/AT.

the blend depends on both the storage modulus and the loss modulus. The loss factor peaks located near  $-60^{\circ}\text{C}$  for PP/EPDM and PP/EPDM/AT systems correspond to the glass transition of EPDM,<sup>5</sup> whereas the dominant loss factor peaks around  $0^{\circ}\text{C}$  for all the blends represent the glass transition of PP.<sup>17</sup> This further proved the “sea-island” morphology of the ternary blends as observed afore. A slight displacement of the glass transition peak of PP to lower temperature was observed as the result of the presence of EPDM with low glass transition temperature ( $T_g$ ). It was also true that the transition peaks of PP in ternary blend became wider and weaker at the higher loading of EPDM. Evidently, the  $T_g$  of the EPDM in PP/EPDM/AT (100/20/5) ternary system was higher than that of PP/EPDM(100/20), and the  $T_g$  transition region of EPDM was broadened. It is explained that, in this system, the incorporation of AT could cause immobilization of part EPDM chains besides free EPDM dispersed particles. This again proved that the morphology structure of PP/EPDM/AT ternary blends was of an encapsulation type, where AT was encapsulated by EPDM. Similar results have been reported for PP/EVA/ $\text{CaCO}_3$  blends with encapsulation structure, in which  $\text{CaCO}_3$  particles was encapsulated by EVA. As a result, the glass transition of EVA was broadened and  $T_g$  shifted towards higher temperature.<sup>18</sup>

At about  $-60^{\circ}\text{C}$ , the loss factor for the PP/EPDM and PP/EPDM/AT blends was higher due to introduction of EPDM, compared with PP. Similarly, the

loss factor for PP/EPDM/AT systems increased with the rising EPDM at the same AT loading but the  $T_g$  of the EPDM little changes. It was abnormal that the loss factor located near  $-60^{\circ}\text{C}$  for PP/EPDM/AT (100/20/5) was evidently higher than that for PP/EPDM (100/20). As we know, the introduction of the inorganic filler can weaken the viscoelasticity of polymer in glassy transition region and therefore lower its loss factor. This phenomenon might be related with the dispersion morphology of AT encapsulated in EPDM.

#### *Impact-fractured morphology*

To understand the toughening mechanism of PP/EPDM/AT ternary blends, the SEM micrographs of impact fracture surface for the PP/EPDM, PP/EPDM/AT are shown in Figure 3a–c respectively. The typical ductile fracture morphology for PP/EPDM blend was observed. As pointed out by Wu,<sup>19</sup> the crazing initiation has been regarded as the well-known mechanism for brittle polymer. PP is brittle polymer with low crack initiation and low crack propagation energies during impact. The rubber particles in matrix may help to initiate the crazings, and terminate the crazings when the rubber particle size is comparable to the crazing thickness. As shown in Figure 3a, a great deal of crazings with tearing pieces were observed on the coarse fracture surface of PP/EPDM sample. Besides the initiation of crazing, the matrix crazings around EPDM particles may encounter each other so as to absorb impact energy. For the

ternary PP/EPDM/AT system, a distinctly different fracture surface were observed in Figure 3b, 3c, where matrix yielding and tearing pieces with dimples on fractured surface was weakened. However, a number of particles embedded in the matrix were detached and interface cavities around them even some small holes were left. These pulled-out particles could be EPDM/AT particles. When the matrix is subject to impact, the cavities formed around particle-polymer boundaries will release the plastic constraint in the matrix and trigger large-scale plastic deformation, significantly improving the fracture toughness of the matrix.<sup>20</sup> For the ternary PP/EPDM/AT system, besides the effect of EPDM, the slippage between AT fibrillar single crystals or loose-stacking crystal bundles during the deformation of dispersed encapsulation particles may absorb energy, resulting in the synergetic improvement of impact strength. On the other hand, due to the incorporation of fibrillar silicate, the stiffness of dispersed encapsulation particles was detrimental to the initiation and extension of matrix crazing. Moreover, when the loading amount of AT was relatively high, the AT agglomerates may act as stress concentration sites to induce the development of the cavities at the particle-polymer boundaries, leading to the reduction of impact strength. Therefore, the micromechanical deformation process-mainly debonding of dispersed particles and shear yielding was mainly responsible for impact resistance of the ternary blends.

## CONCLUSIONS

It was concluded that the morphology of encapsulation structure like sandbag was formed in PP matrix besides neat EPDM dispersion phase, where EPDM encapsulated fibrillar silicate attapulgite (AT), via two-step melt blending process. Meantime, as for PP/EPDM/AT ternary blends, the typical “sea-island” morphology was observed, and the most-odds diameter ( $D_m$ ), the number-average diameter ( $D_n$ ) and the weight-average diameter ( $D_w$ ) of the dispersed particles in ternary blends decreased with increasing EPDM. PP/EPDM/AT ternary blends showed higher yield strength and dynamic modulus than the corresponding PP/EPDM binary systems due to the reinforcement of AT. PP/EPDM/AT ternary blend (100/

20/5) possessed the balanced yield strength (21.9 MPa) and impact strength ( $47.7 \text{ kJ}\cdot\text{m}^{-2}$ ), relative to 23.0 MPa and  $9.4 \text{ kJ}\cdot\text{m}^{-2}$  of PP. The micromechanical deformation process-mainly debonding of dispersed particles and shear yielding was mainly responsible for impact resistance of the ternary blends.

*Acknowledgment.* The authors gratefully thank Ministry of Science and Technology of China (2002AA334050) as well as Beijing Municipal New Star Plan Project (H020820620120) for financial support.

## REFERENCES

1. W. Jiang, S. C. Tjong, and R. K. Y. Li, *Polymer*, **44**, 3479 (2000).
2. A. L. N. da Silva and F. M. B. Coutinho, *Polym. Test.*, **15**, 45 (1996).
3. J. E. Stamhius, *Polym. Compos.*, **9**, 72 (1988).
4. J. E. Stamhius, *Polym. Compos.*, **9**, 280 (1988).
5. J. Kolaric and J. Jancar, *Polymer*, **33**, 4961 (1992).
6. J. Kolaric, B. Pukansky, and F. Lednický, *Compos. Polym. Commun.*, **2**, 271 (1990).
7. K. Schaefer, A. Theinsen, M. Hess, and R. Kosfeld, *Polym. Eng. Sci.*, **33**, 1009 (1993).
8. J. Zhou, N. Liu, and Y. Li, *et al.*, *Silicate Bulletin*, **6**, 50 (1999).
9. H. H. Murray, *Appl. Clay Sci.*, **17**, 207 (2000).
10. M. Tian, C. D. Qu, L. Q. Zhang, and Y. Feng, *J. Mater. Sci.*, **38**, 4917 (2003).
11. Z. J. Du, J. F. Rong, H. Q. Li, W. Zhang, and Z. Jing, *J. Mater. Sci.*, **38**, 4863 (2003).
12. E. N. Brown, A. K. Davis, K. D. Jonnalagadda, and N. R. Sottos, *Compos. Sci. Technol.*, **65**, 129 (2005).
13. T. K. Kang, Y. Kim, W. K. Lee, H. D. Park, W. J. Cho, and C. S. Ha, *J. Appl. Polym. Sci.*, **72**, 989 (1999).
14. Béla Pukánszky, F. Tüdös, Jan Kolařík, František Lednický, *Polym. Compos.*, **11**, 98 (1990).
15. J. Kolarik, B. Pukanszky, and F. Lednický, in “Interfaces in Polymer, Ceramics, and Metal Matrix Blends” H. Ishida Ed., Elsevier, 1988, p 453.
16. G. H. Michler and J. M. Tovmasjan, *Plaste Kautsch.*, **35**, 73 (1988).
17. Q. Baigong, in “Transition and Relaxation of Polymers,” Science Press, Beijing, 1986, pp 365–366.
18. K. Premphet and P. Horanont, *Polymer*, **41**, 9283 (2000).
19. W. Souheng, *Polymer*, **26**(11), 1855 (1985).
20. S. Molnar, B. Pukanszky, and C. O. Hammer, *Polymer*, **41**, 1529 (2000).